Supplementary Information

Bridged emulsion gels from polymer–nanoparticle enabling large-amount biomedical encapsulation and functionalization

Chuchu Wan[1], Si He[2], Quanyong Cheng[1], Kehan Du[1], Yuhang Song[1], Xiang Yu[1], Hao Jiang[1], Caili Huang[1], Jiangping Xu[1], Cong Ma[2], and Jintao Zhu[1]*

[1] Key Laboratory of Materials Chemistry for Energy Conversion and Storage of Ministry of Education (HUST), School of Chemistry and Chemical Engineering, Huazhong University of Science and Technology (HUST), Wuhan 430074, China

[2] Key Laboratory of Molecular Biophysics of the Ministry of Education (HUST), College of Life Science and Technology, Huazhong University of Science and Technology (HUST), Wuhan, 430074, China

***Corresponding Author**

E-mail: cailihuang@hust.edu.cn (Caili Huang)

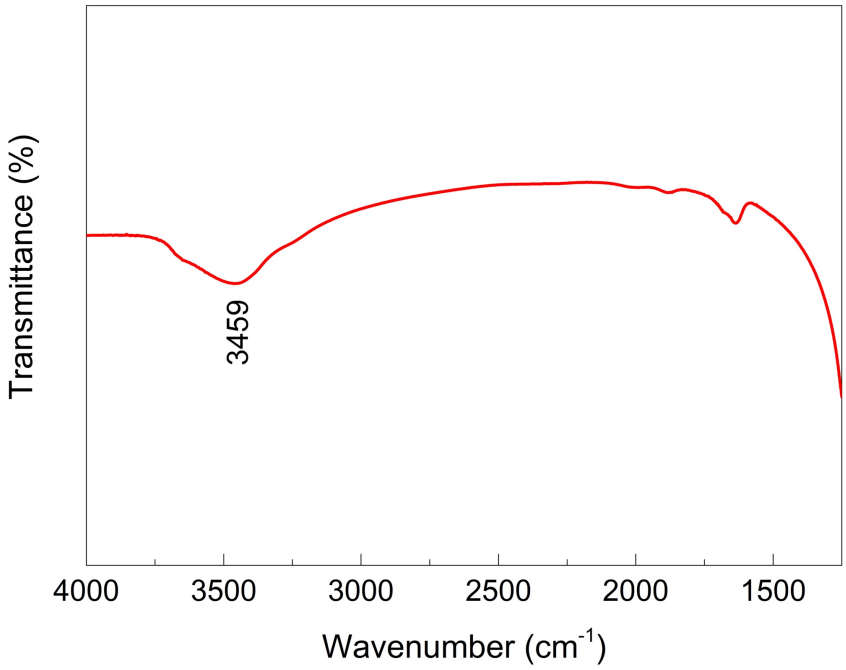

Supplementary Fig. 1. Fourier transform infrared (FTIR) spectra of the commercial SiO_2 NPs, the peak at 3459 cm^{-1} corresponds to the −OH group on the surface of the NPs.

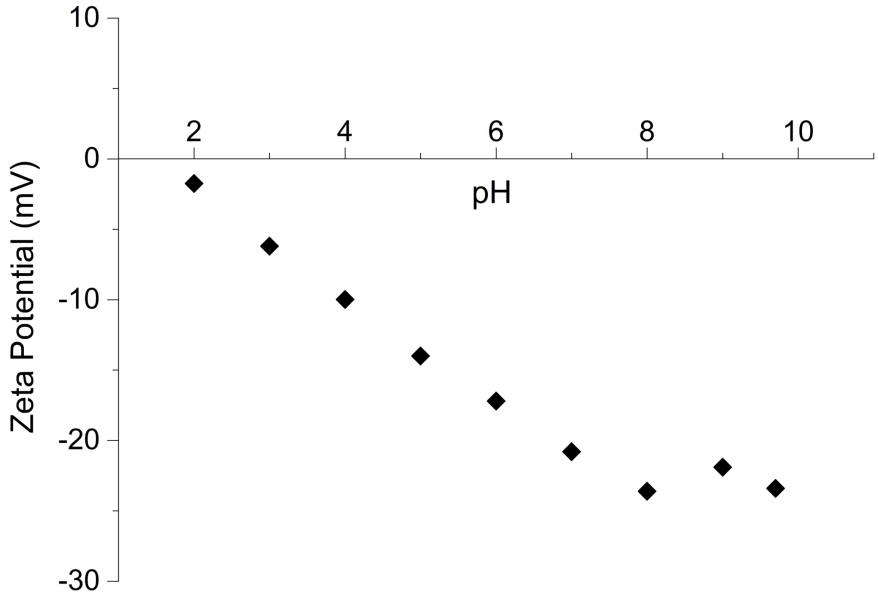

Supplementary Fig. 2. Zeta potential as a function of pH for aqueous suspensions of commercial SiO_2 NPs (1 mg mL^{-1}).

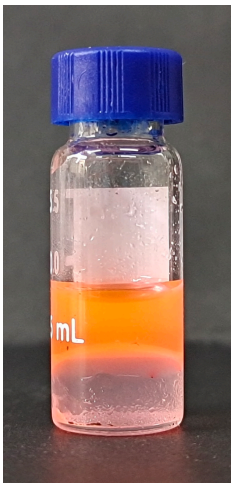

Supplementary Fig. 3. Photo of the mixture (recorded after 5 min) with equal volumes of water and toluene solution of PDMS-NH_2 (3% *w*/*w*).

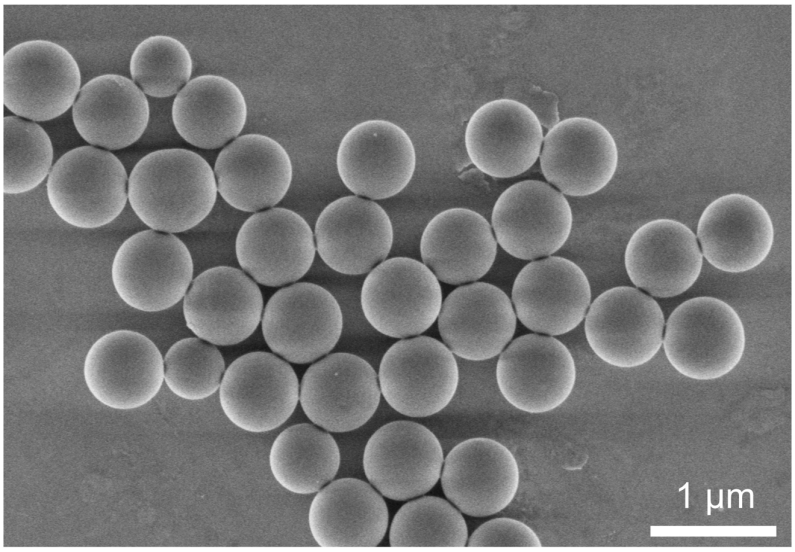

Supplementary Fig. 4. Scanning electron microscopy (SEM) image of synthetic RITC-tagged SiO_2 NPs. The average diameter of the NPs is 630 nm.

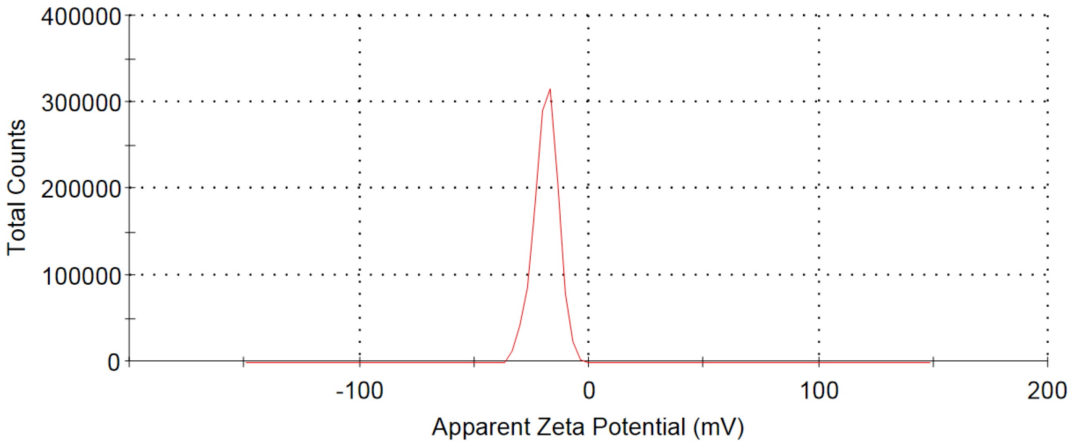

Supplementary Fig. 5. Zeta potential for aqueous suspension of synthetic RITC-tagged SiO_2 NPs (1 mg mL^{-1}, pH = 7, –18.8 mV).

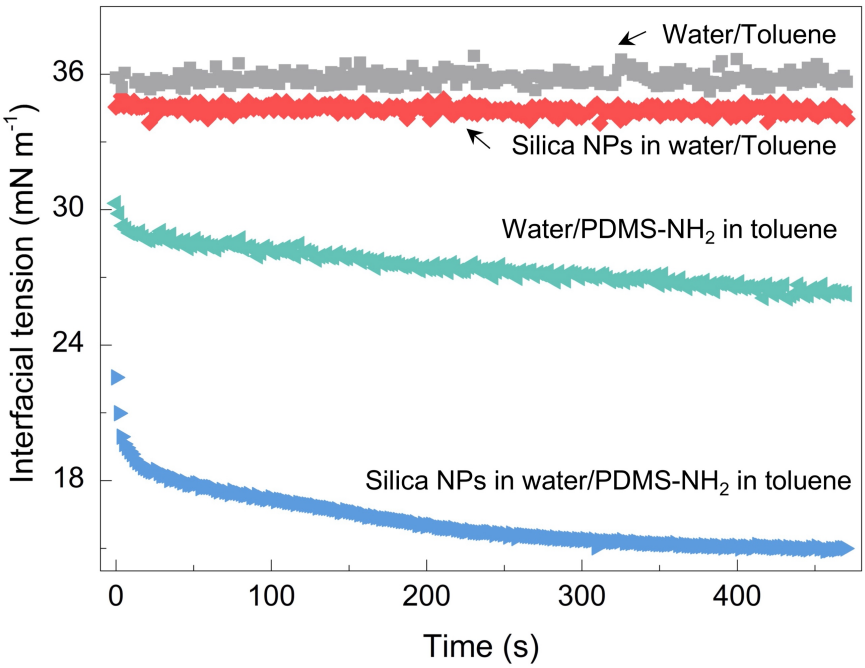

Supplementary Fig. 6. The recruitment of synthetic RITC-tagged SiO_2 NPs to the interfaces by PDMS-NH_2 occurs on different time scales and depends on the relative concentration of each. These processes can be observed by monitoring the interfacial tension as a function of time for a pendant water drop suspended in a bath of toluene for systems configured with either nothing (gray squares), RITC-tagged SiO_2 NPs (red rhombuses), PDMS-NH_2 (green triangles), or RITC-tagged SiO_2 NPs + PDMS-NH_2 (blue triangles). The concentration of RITC-tagged SiO_2 NPs in water is 2% *w*/*w* and the concentration of PDMS-NH_2 in toluene is 0.05% *w*/*w*.

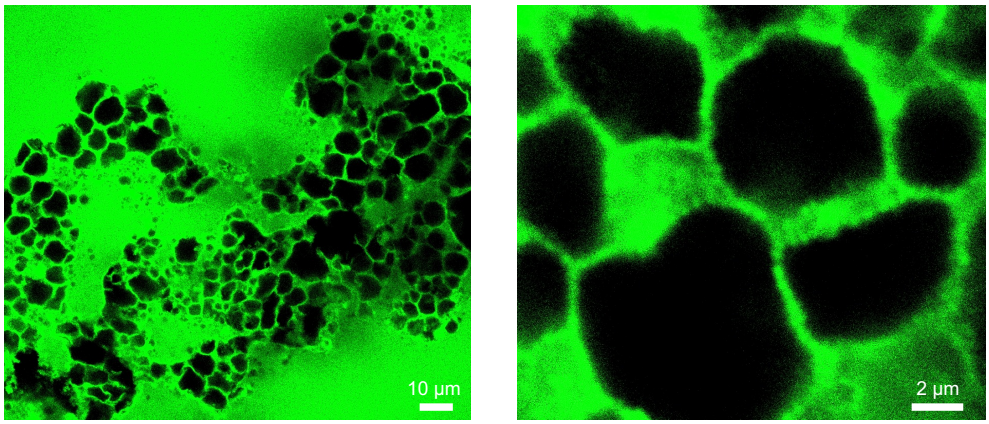

Supplementary Fig. 7. Low-magnification and high-magnification confocal microscopy images of the o/w bridged emulsion gel as the aqueous phase is stained with rhodamine B. [RITC-tagged SiO_2 NPs] = 8% *w*/*w*, [PDMS-NH_2] = 3% *w*/*w*, water/oil ratio is 5:5 (*v*/*v*).

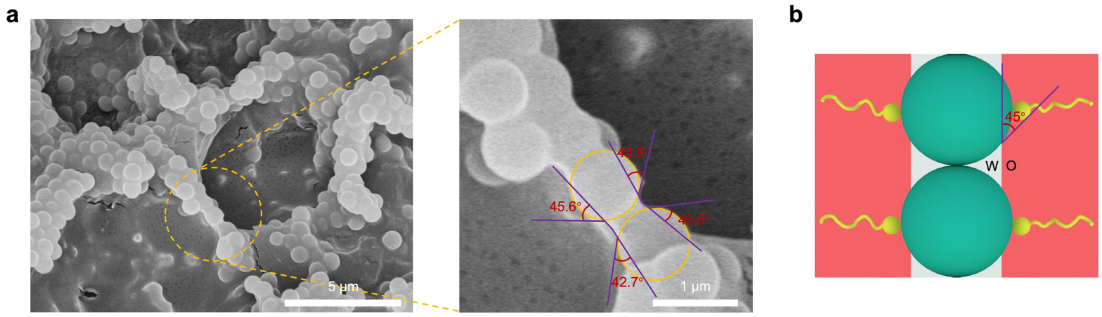

Supplementary Fig. 8. a Cryo-scanning electron microscopy (cryo-SEM) images of the o/w bridged emulsion gel demonstrating the three-phase contact angle of the NPs between the closely neighbored droplets. [RITC-tagged SiO_2 NPs] = 8% *w*/*w*, [PDMS-NH_2] = 3% *w*/*w*, water/oil ratio is 5:5 (*v*/*v*). The average diameter of the NPs is 630 nm. The oil phase is selectively removed in the cryo-electron microscopy testing. The solid yellow lines depict the contours of the NPs, the solid purple lines depict the interface between the water and the oil phase, thus the three-phase contact angle of the NPs is acquired at ~ 45° [44.6° = (43.5° + 46.6° + 42.7° + 45.6°)/4, with respect to the water phase]. **b** Schematic representation of an o/w bridged emulsion gel prepared by the NPs with 45° (with respect to the water phase, regulated by polymers) spanning the interfaces of two oil droplets. The green balls represent the NPs, the yellow chains represent the polymers, and the white and red phases represent the water and the oil phases, respectively.

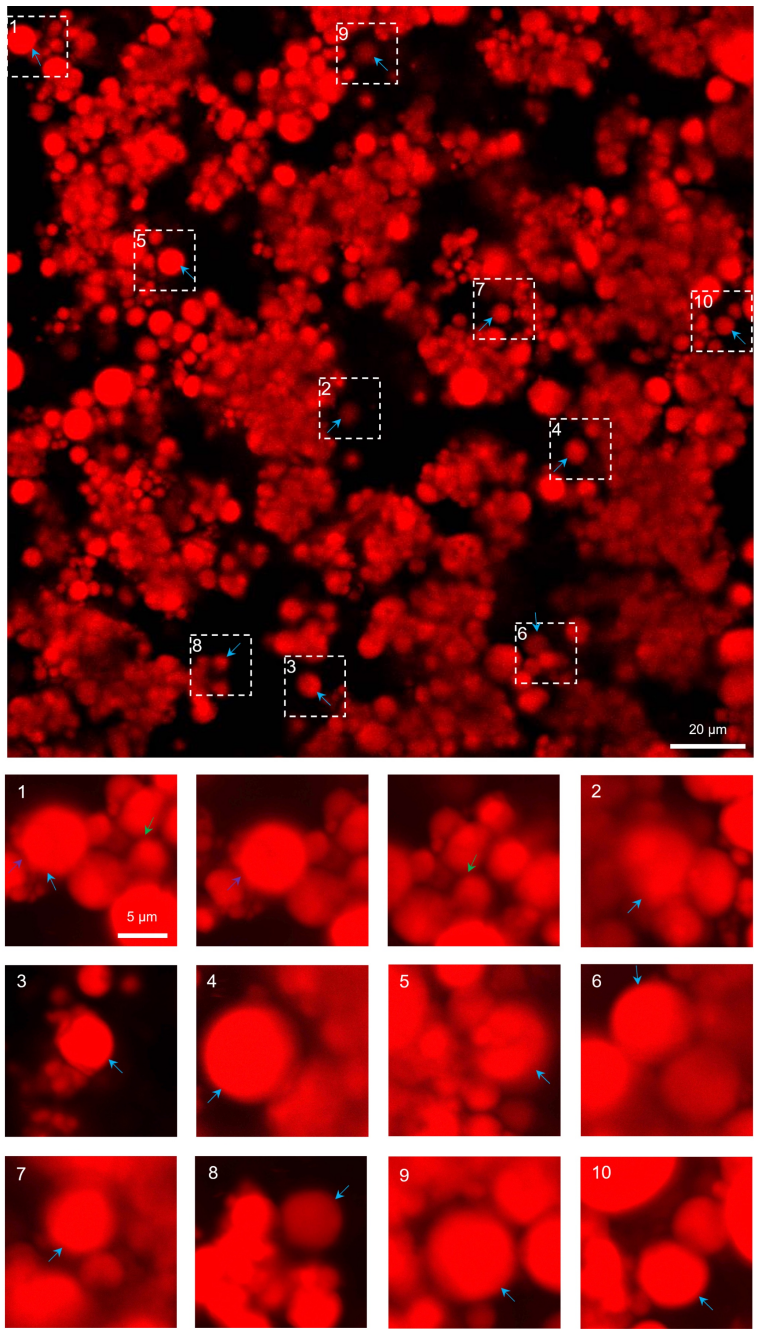

Supplementary Fig. 9. A confocal image and the corresponding 12 zoomed-in images of emulsion gels formed by polymer–NP ensembles. [SiO_2 NPs] = 4% *w*/*w*, [PDMS-NH_2] = 3% *w*/*w*, water/oil ratio is 5:5 (*v*/*v*). To clearly visualize the three-dimensional structure of the emulsion gels, some zoomed-in images have been refocused (To view the interface, certain droplets are not clear). The white dotted box shows the zoomed-in area. The blue arrow shows the same droplet before and after zoomed-in, and the purple and green arrows mark the same boundaries.

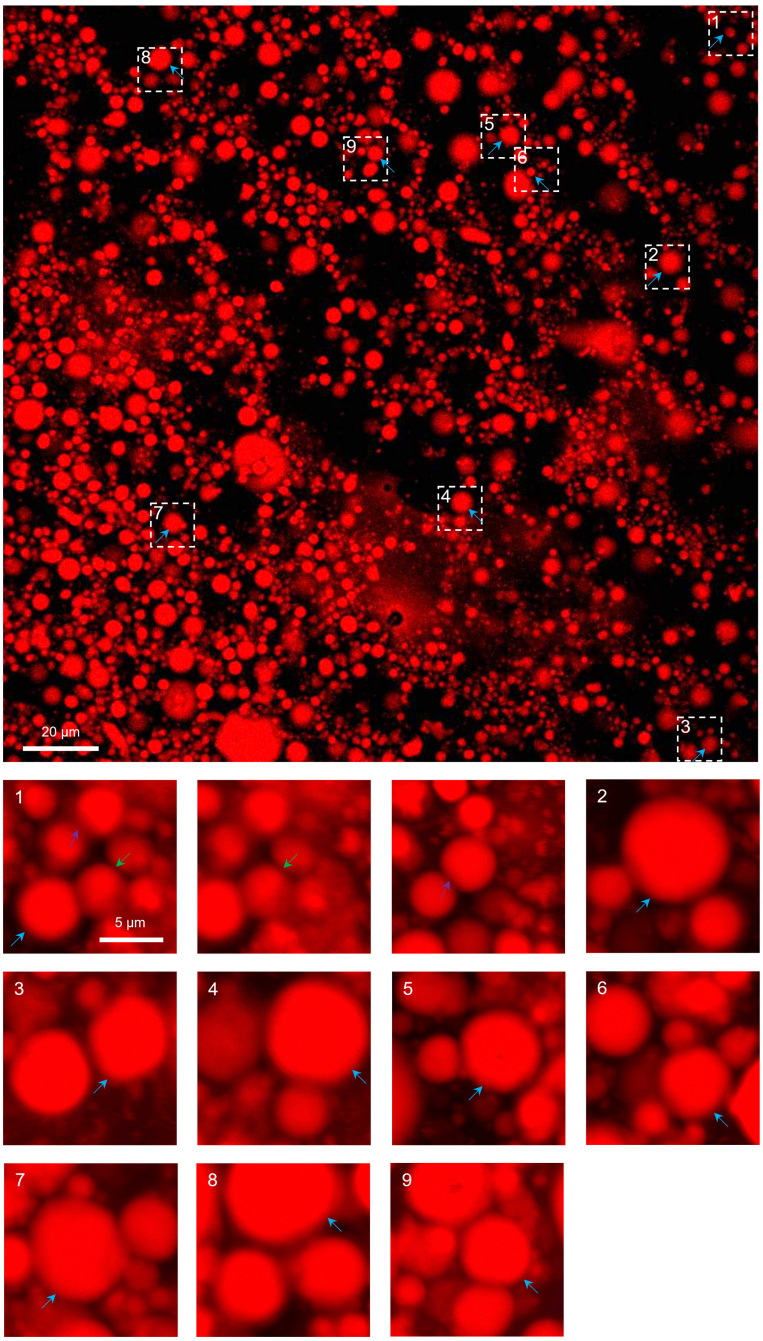

Supplementary Fig. 10. A confocal image and the corresponding 11 zoomed-in images of emulsion gels formed by polymer–NP ensembles. [SiO_2 NPs] = 8% *w*/*w*, [PDMS-NH_2] = 3% *w*/*w*, water/oil ratio is 5:5 (*v*/*v*). The white dotted box shows the zoomed-in area. The blue arrow shows the same droplet before and after zoomed-in, and the purple and green arrows mark the same boundaries.

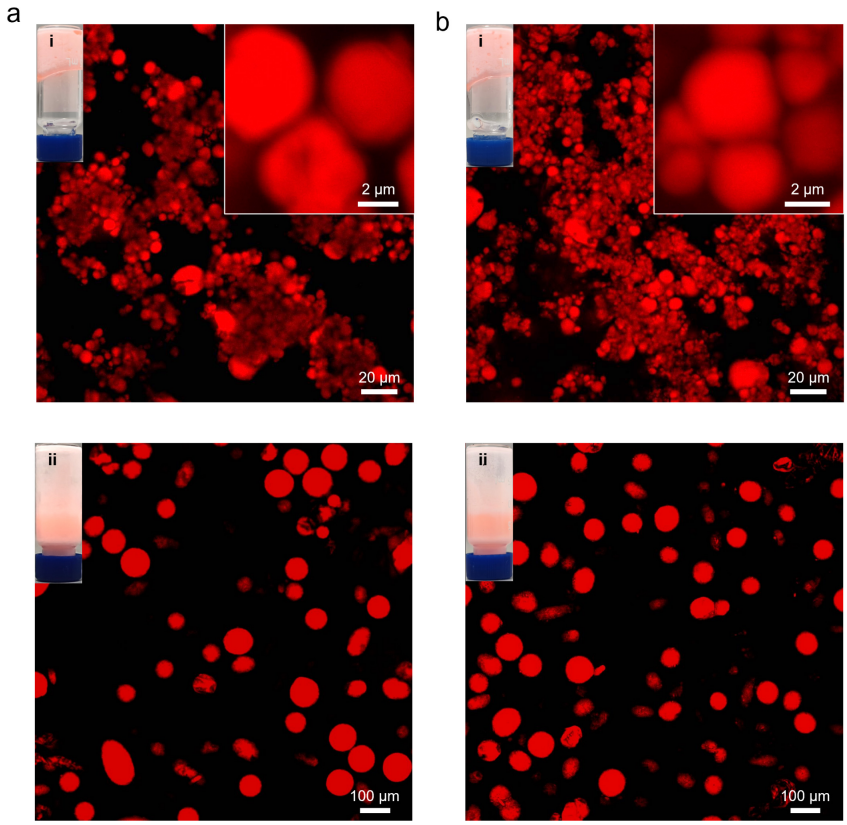

Supplementary Fig. 11. a Confocal microscopy images of samples that prepared *via* (i) ultrasonication (46 W for 14 s continuously) and (ii) vortex mixing (3,000 rpm for 5 min). [SiO_2 NPs] = 4% *w*/*w*, [PDMS-NH_2] = 3% *w*/*w*, water/oil ratio is 5:5 (*v*/*v*). **b** Confocal microscopy images of samples that prepared *via* (i) ultrasonication (46 W for 14 s continuously) and (ii) vortex mixing (3,000 rpm for 5 min). [SiO_2 NPs] = 8% *w*/*w*, [PDMS-NH_2] = 3% *w*/*w*, water/oil ratio is 5:5 (*v*/*v*). Inset showing the macroscopic appearance of the emulsions.

Ultrasonication treatment yields highly stable and bridged emulsion gels composed of faceted droplet clusters regardless of NP's concentration, whereas vortex mixing produces common emulsions composed of spherical, isolated, and sparse droplets. And, the droplet size of the bridged emulsion gels is much smaller than that of the common emulsions. The reason that the two shear forces generate totally different morphologies of the emulsion can be found in the evolution and formation process of emulsions. Firstly, the emulsions evolved procedures that include: emulsion droplet generation upon oil/water mixing, polymer/NP assembly, droplet collision and coalescence until

the system is trapped by the jamming of the interfacial NPs. Secondly, ultrasonication has much stronger shear force than vortex, such that the former will lead to much more, smaller droplets. As described in the Results and Discussion Section, a relatively low amount of polymers recruits the NPs to assemble at the interfaces, where the NPs have a low three-phase contact angle with respect to the aqueous phase, along with the evolution of the small, emulsified droplets (capillary bridge formation and coalescence), leading to the jamming of bridged emulsions, i.e., forming the bridged emulsion gels. In contrast, vortex mixing generates much fewer, larger droplets, such that less droplet collision happens, and it will allow the isolate droplets to have enough time to be covered by the polymer–NP assemblies, thus preventing further Ostwald Ripening.

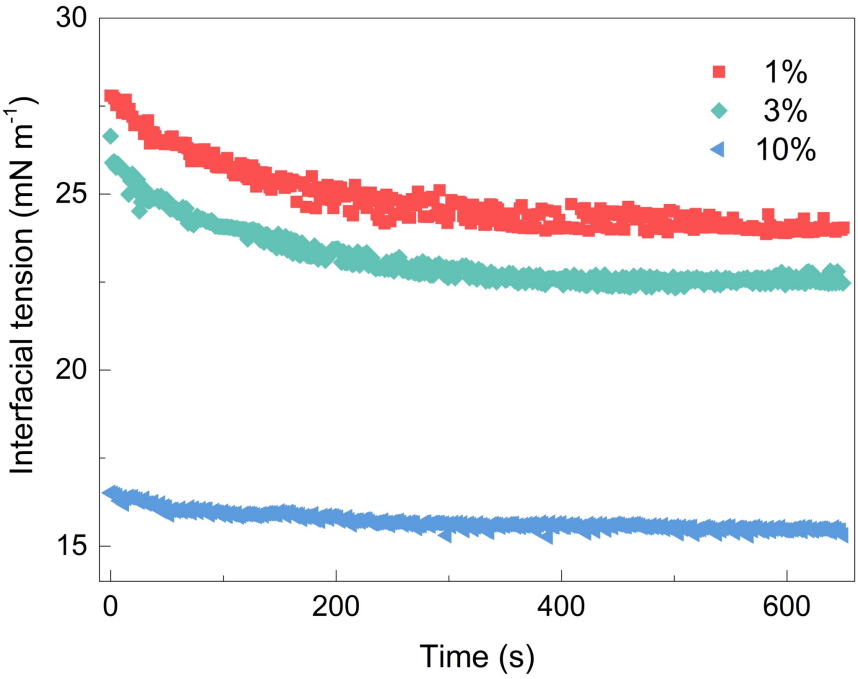

Supplementary Fig. 12. Dynamic interfacial tension of pure water in contact with toluene solutions of PDMS-NH_2 in different concentrations (*w*/*w*).

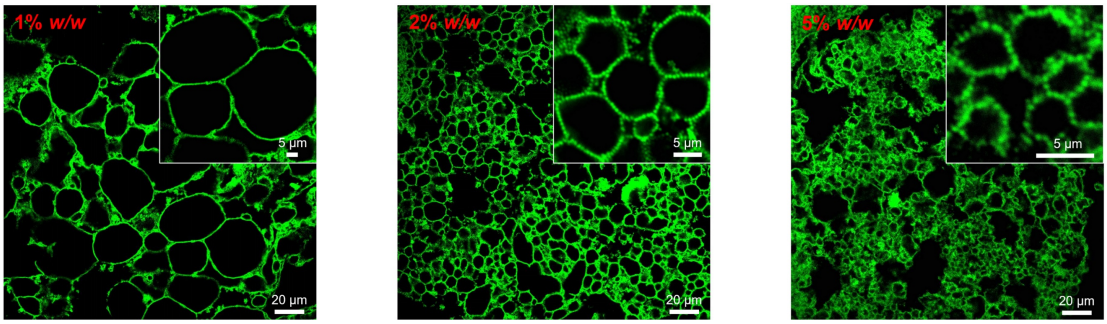

Supplementary Fig. 13. Low-magnification and high-magnification confocal microscopy images of bridged emulsion gels prepared over a broad range of PDMS-NH_2 concentrations (1%–5% *w*/*w*) showing a monolayer of particles bridging numbers of faceted droplets in the gel interior as the particles are tagged with RITC. [SiO_2 NPs] = 8% *w*/*w*, water/oil ratio is 5:5 (*v*/*v*). Note that variation of PDMS-NH_2 loading has substantial impact on emulsion gels' droplet size for the large NPs compared to the Ludox small NPs, which can be attributed to the former's much slower diffusion to the interfaces.

The polymer chain number (in our experimental range) only impacts the initial speed of polymers approaching the interfaces, but does not vary the final microstructures (or morphologies), i.e., their 45° contact angle, such that higher polymer concentration condition leads to smaller emulsion droplets based gels. Naturally, large NPs have different ranges of polymer concentration with smaller Ludox NPs, due to the different effective number chains to form 45° contact angle.

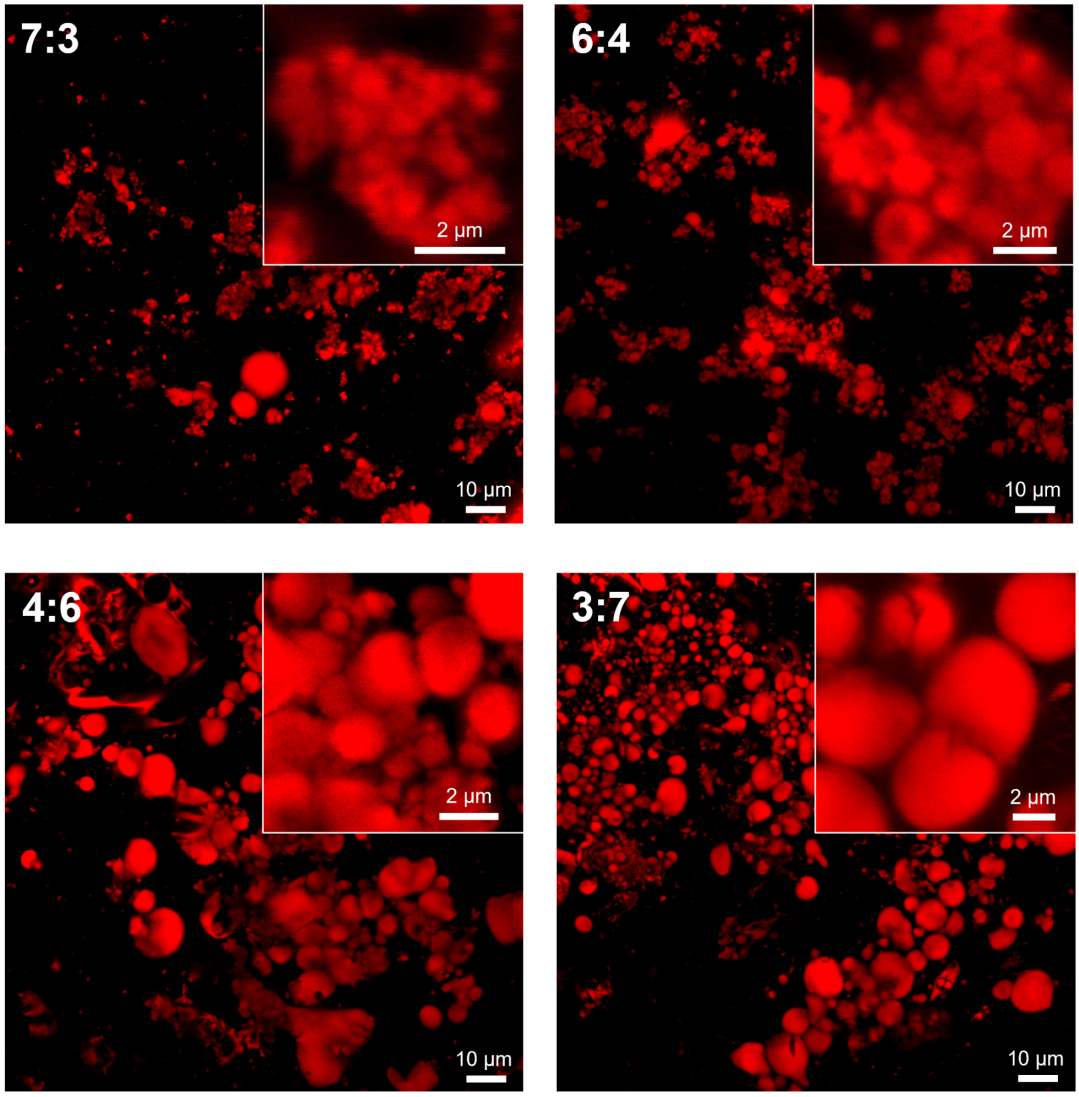

Supplementary Fig. 14. Confocal microscopy images of bridged emulsion gels formed by polymer–NP ensembles with the volume ratio of the water to the oil phase from 7:3 to 3:7. [SiO_2 NPs] = 4% *w*/*w*, [PDMS-NH_2] = 3% *w*/*w*. The average droplet diameter: 1.4 ± 0.5 µm (7:3 water/oil volume ratio), 1.8 ± 0.8 µm (6:4 water/oil volume ratio), 5.8 ± 1.4 µm (4:6 water/oil volume ratio), 5.9 ± 1.6 µm (3:7 water/oil volume ratio).

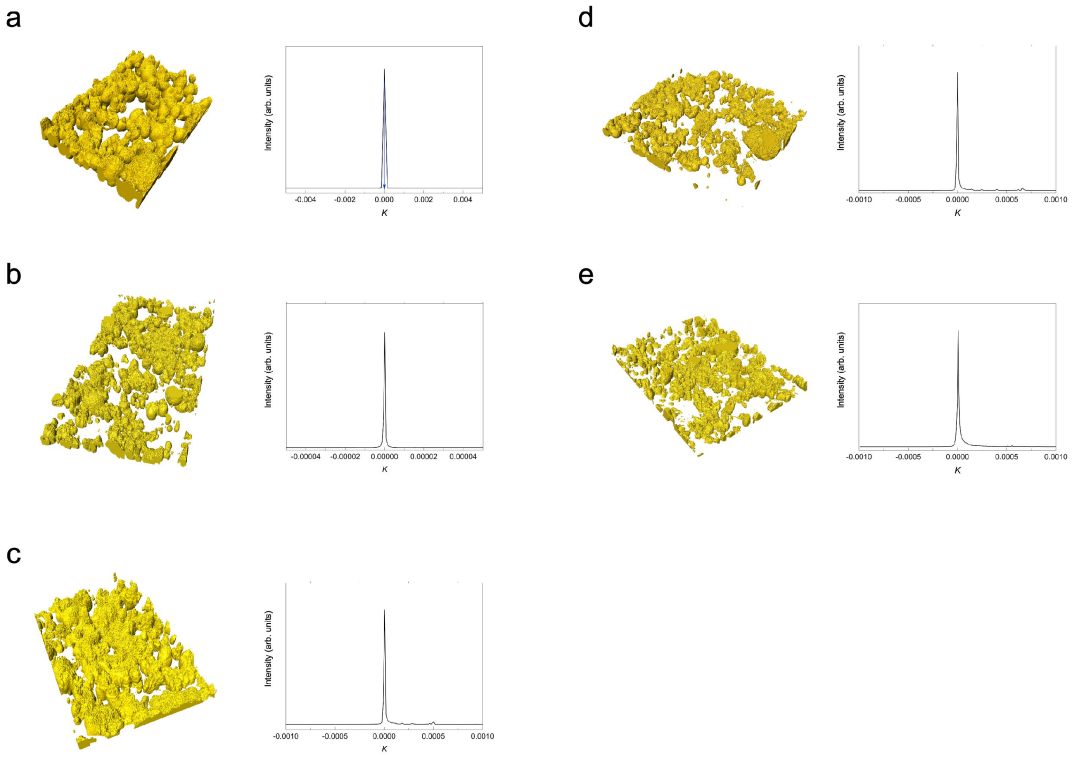

Supplementary Fig. 15. The Gaussian curvature distributions and the corresponding surface reconstructions of emulsion gel samples in Fig. 2 and Fig. 1c. **a** [SiO_2 NPs] = 2% *w*/*w*, [PDMS-NH_2] = 3% *w*/*w*, water/oil ratio is 5:5 (*v*/*v*). **b** [SiO_2 NPs] = 4% *w*/*w*, [PDMS-NH_2] = 3% *w*/*w*, water/oil ratio is 5:5 (*v*/*v*). **c** [SiO_2 NPs] = 8% *w*/*w*, [PDMS-NH_2] = 3% *w*/*w*, water/oil ratio is 5:5 (*v*/*v*). **d** [SiO_2 NPs] = 4% *w*/*w*, [PDMS-NH_2] = 1% *w*/*w*, water/oil ratio is 5:5 (*v*/*v*). **e** [SiO_2 NPs] = 4% *w*/*w*, [PDMS-NH_2] = 3% *w*/*w*, water/oil ratio is 8:2 (*v*/*v*).

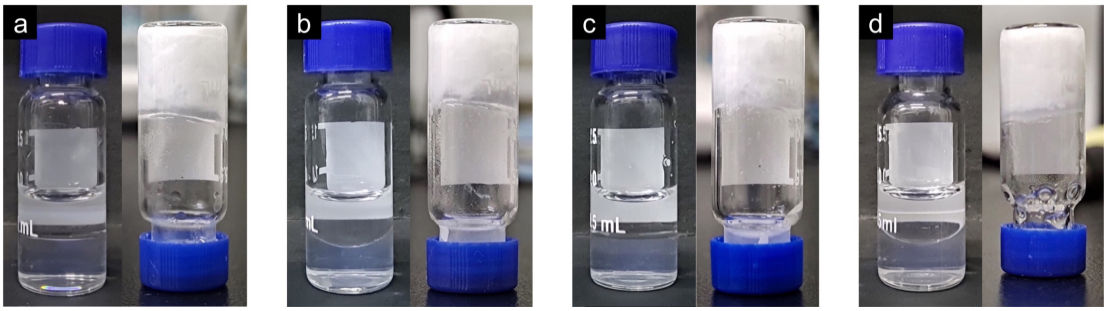

Supplementary Fig. 16. Photos of bridged emulsion gels prepared using different functional polymers, such as **a** PS-NH_2, different oil phases, such as **b** olive oil, **c** *n*-hexane, and **d** tricaprylin.

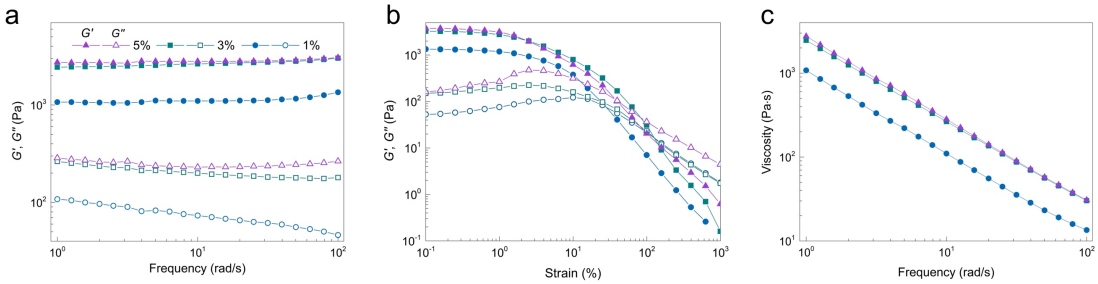

Supplementary Fig. 17. a Frequency sweeps of storage modulus G' and loss modulus G'' of bridged emulsion gels with different polymer concentrations. [SiO_2 NPs] = 4% *w*/*w*, water/oil ratio is 5:5 (*v*/*v*). The strain is kept constant at 1%. **b** Strain sweeps of G' and G'' of bridged emulsion gels with different polymer concentrations. [SiO_2 NPs] = 4% *w*/*w*, water/oil ratio is 5:5 (*v*/*v*). The frequency is kept constant at 10 rad s^{-1}. **c** Frequency sweeps of viscosity of bridged emulsion gels with different polymer concentrations. [SiO_2 NPs] = 4% *w*/*w*, water/oil ratio is 5:5 (*v*/*v*). The strain is kept constant at 1%.

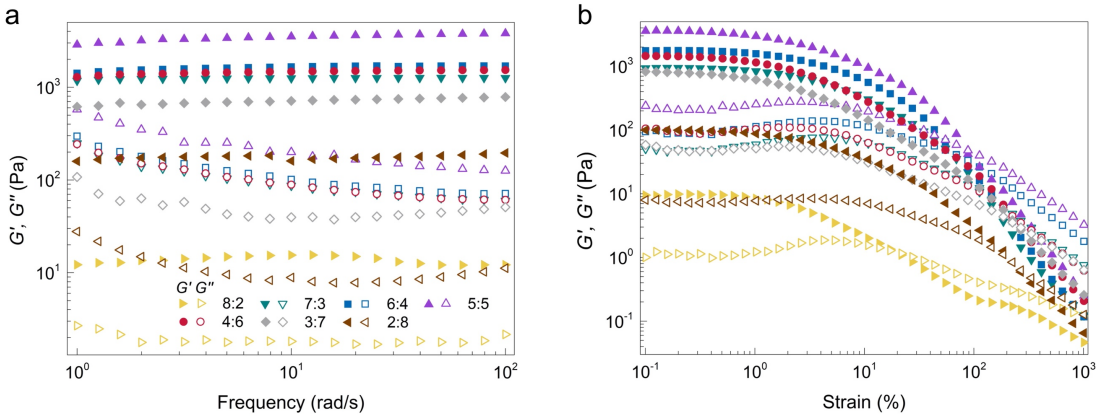

Supplementary Fig. 18. a Frequency sweeps of G' and G'' of bridged emulsion gels with different volume ratios of the water to the oil phase varying from 8:2 to 2:8. [SiO_2 NPs] = 4% *w*/*w*, [PDMS-NH_2] = 3% *w*/*w*. The strain is kept constant at 1%. **b** Strain sweeps of G' and G'' of bridged emulsion gels with different volume ratios of the water to the oil phase varying from 8:2 to 2:8. [SiO_2 NPs] = 4% *w*/*w*, [PDMS-NH_2] = 3% *w*/*w*. The frequency is kept constant at 10 rad s^{-1}.

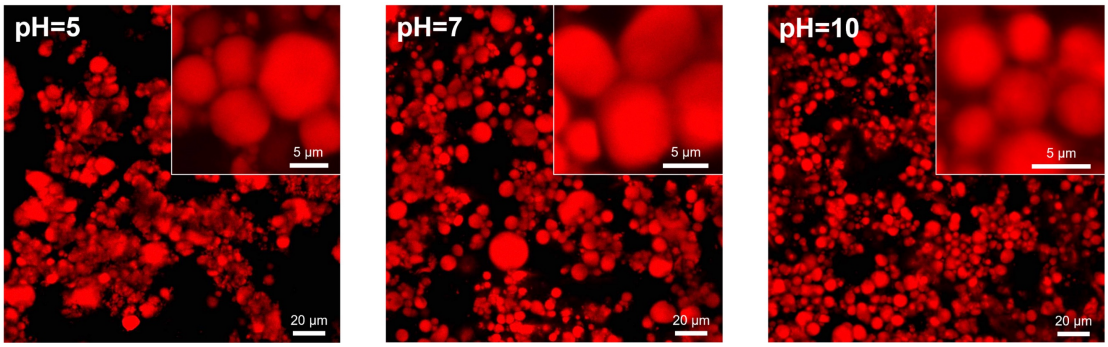

Supplementary Fig. 19. Bridged emulsion gel systems formed by polymer–NP ensembles at different pH. [SiO_2 NPs] = 4% *w*/*w*, [PDMS-NH_2] = 3% *w*/*w*, water/oil ratio is 5:5 (*v*/*v*).

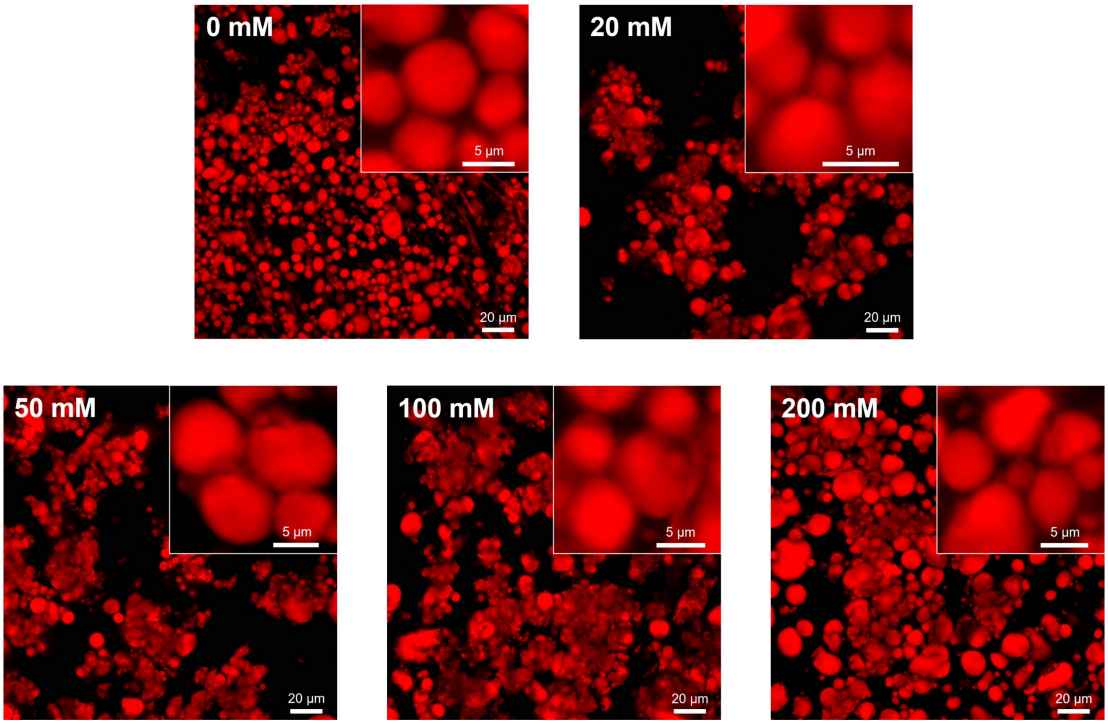

Supplementary Fig. 20. Bridged emulsion gel systems formed by polymer–NP ensembles with different ionic strengths (NaCl). [SiO_2 NPs] = 4% *w*/*w*, [PDMS-NH_2] = 3% *w*/*w*, water/oil ratio is 5:5 (*v*/*v*).

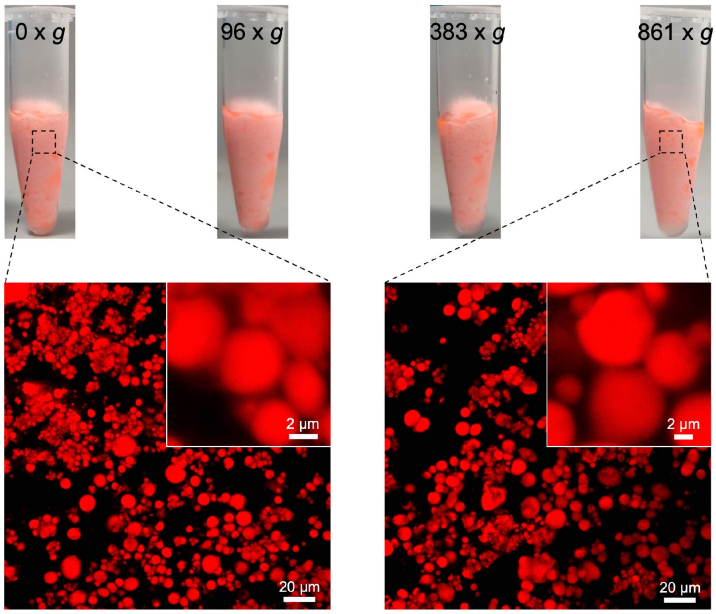

Supplementary Fig. 21. Bridged emulsion gels are stable against centrifugation.

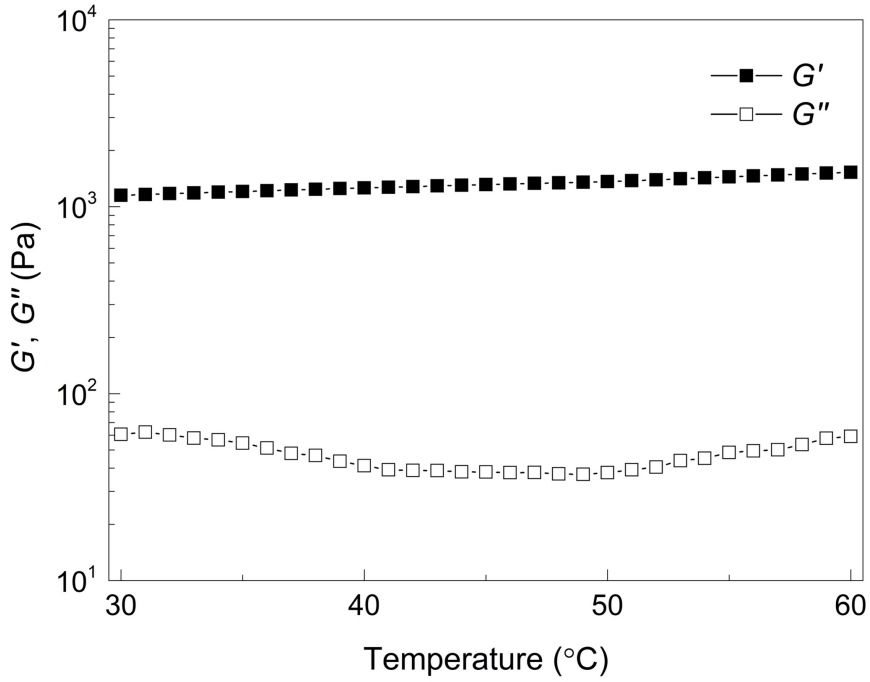

Supplementary Fig. 22. Temperature sweeps of *G′* and *G″* of bridged emulsion gels, which show little temperature dependence. [SiO_2 NPs] = 4% *w*/*w*, [PDMS-NH_2] = 3% *w*/*w*, water/oil ratio is 5:5 (*v*/*v*). The strain is kept constant at 1% and the frequency is kept constant at 10 rad s^{-1}.

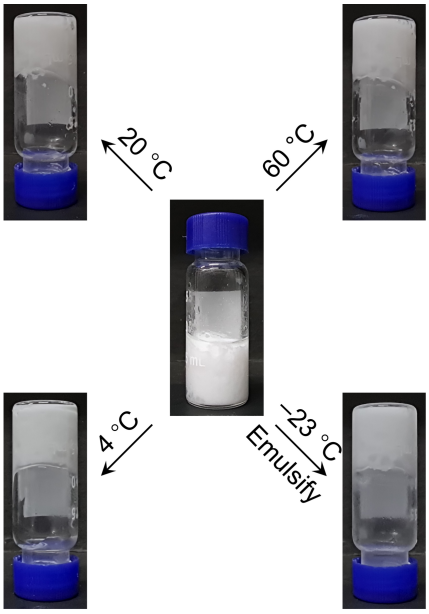

Supplementary Fig. 23. Bridged emulsion gels are stable above freezing point tested at 4 °C, 20 °C, and 60 °C. Bridged emulsion gels are destroyed when stored below freezing point (–23 °C) but can be recovered by re-homogenization.

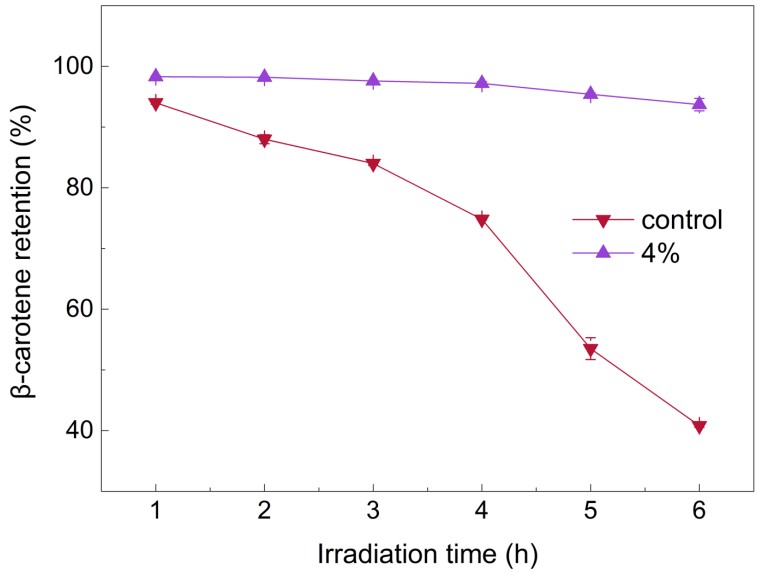

Supplementary Fig. 24. The retention of encapsulated β-carotene in bridged emulsion gels under ultraviolet irradiation. [SiO_2 NPs] = 4% *w*/*w*, [PDMS-NH_2] = 3% *w*/*w*, water/oil ratio is 3:7 (*v*/*v*). Bulk oil loaded with the same content of β-carotene served as the control. Data are presented as mean values ± SD (*n* = 3).

For the control sample, the retention of β-carotene decreased significantly over irradiation time and was less than 41.0% after 6 h, suggesting a continuous, strong ultraviolet (UV) degradation of β-carotene. In stark contrast, β-carotene encapsulated in bridged emulsion gels exhibited enhanced UV stability with a retention of 93.7% following a 6 h duration of UV exposure. In the emulsion gel system, the jamming interfacial layer of polymer–NP ensembles enclosed the β-carotene within oil droplets and impeded direct UV irradiation, thereby significantly diminishing the likelihood of β-carotene degradation.

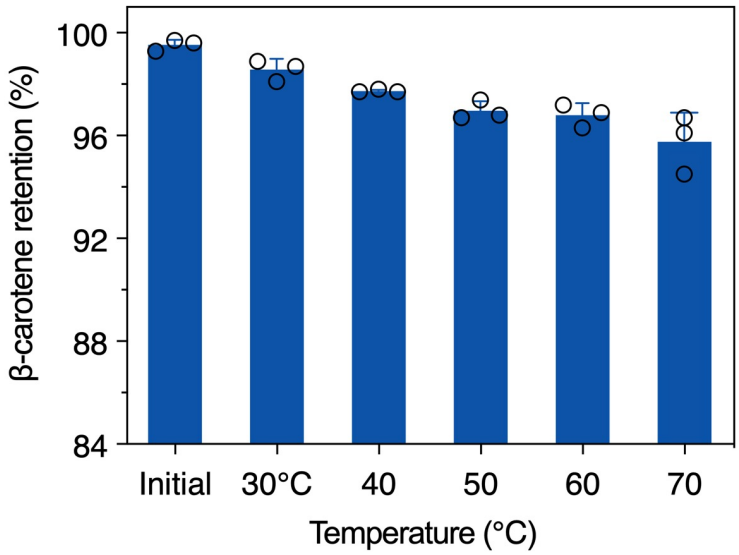

Supplementary Fig. 25. The retention of encapsulated β-carotene in bridged emulsion gels under different temperatures for 30 min. [SiO_2 NPs] = 4% *w*/*w*, [PDMS-NH_2] = 3% *w*/*w*, water/oil ratio is 3:7 (*v*/*v*). Data are presented as mean values ± SD (*n* = 3).

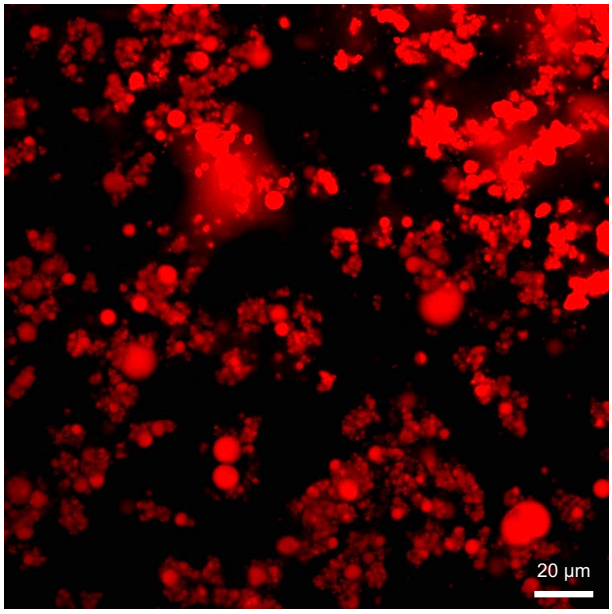

Supplementary Fig. 26. Confocal microscopy image of bridged emulsion gel loaded with anti-sunburn compounds.

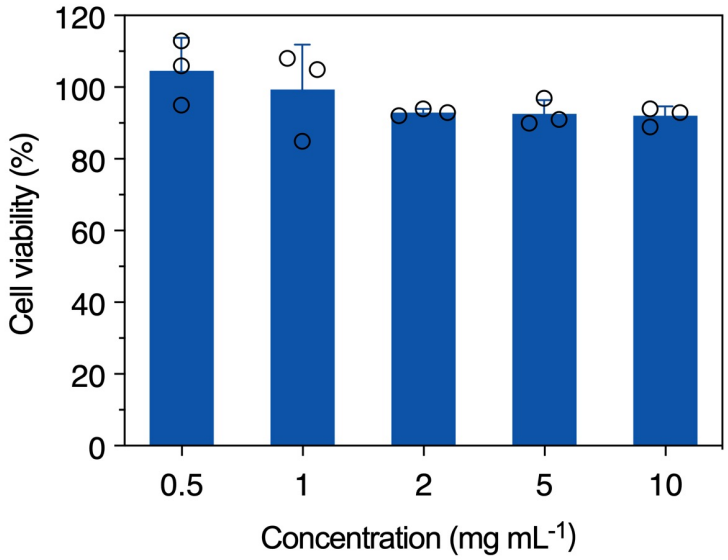

Supplementary Fig. 27. Cell viability (%) for the human keratinocyte cell line (HaCaT cell) after 24 h incubation with emulsion gels of different concentrations. Data are presented as mean values ± SD (n = 3).

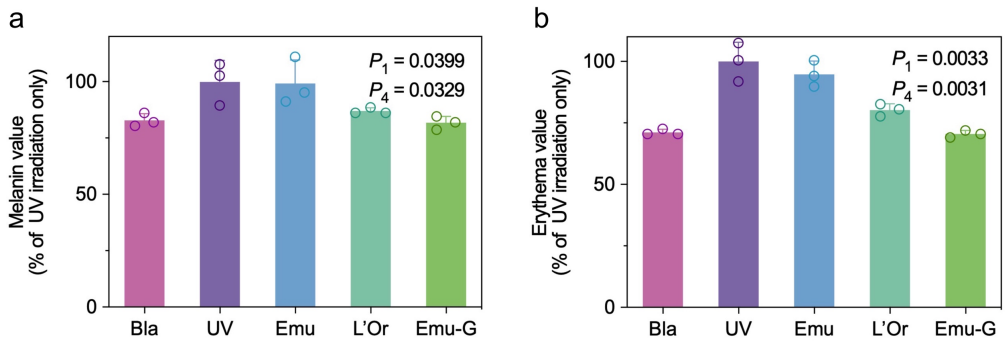

Supplementary Fig. 28. a Relative melanin value of mouse skin swabbed with different protective samples followed by UV irradiation. **b** Relative erythema value of mouse skin swabbed with different protective samples followed by UV irradiation. Data were collected based on the normalization of the UV group (UV irradiation only sample) as 100% and presented as mean ± SD of $n = 3$ biologically independent mice. *P* value showing the statistically significant difference between the two sets of values, consistent with Fig. 5 in the manuscript. Bla represents the blank group, that mice were neither coated with samples nor irradiated with UV spot. UV represents the UV group, that mice were treated with UV irradiation. Emu, L'Or, and Emu-G represent the emulsion, L'Oreal and emulsion gel groups, that mice were swabbed with the same amount of emulsion, L'Oreal sunscreen, and emulsion gel sample before UV irradiation, respectively.

It was found that the mouse skin was severely damaged after UV irradiation without any protection, exhibiting much higher levels of melanin and erythema (from 83% to 100%, and from 71% to 100%, respectively). For the emulsion group, there was still a large amount of melanin and erythema (99% and 95%, respectively), showing negligible protection on the skin due to the encapsulated active substances' quickly flowing away. The melanin and erythema values were reduced when the L'Oreal sunscreen was applied (87% and 80%, respectively), showing a certain protection on the skin. More importantly, the melanin and erythema values of the skins of protected mice by emulsion gels (82% and 71%, respectively) were almost identical to the values of the blank group, indicating their effective resistance to strong UV exposure.

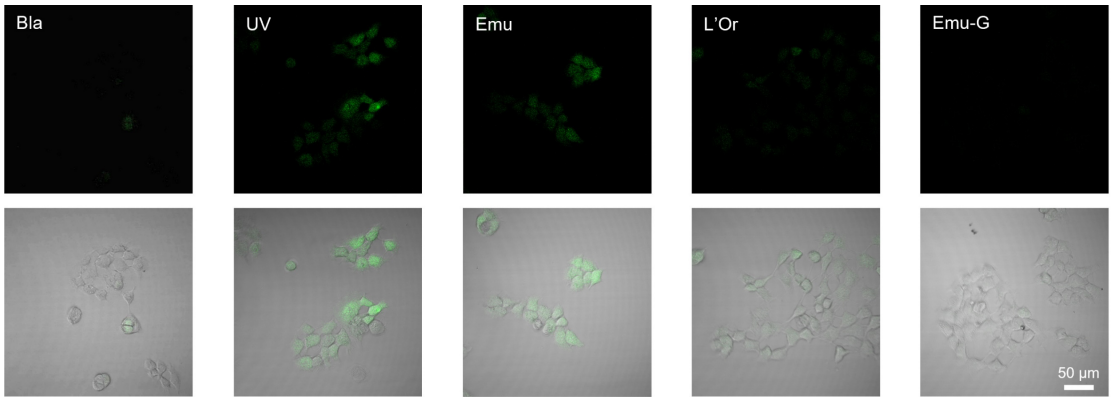

Supplementary Fig. 29. Fluorescent confocal microscope images of HaCaT cells covered with different protective samples followed by UV irradiation and incubating with oxidation-sensitive fluorescent probe (carboxy-H2DCFDA), showing reactive oxygen species (ROS) generation and in vitro UV protection effect. Bla represents the blank group, that cells were neither covered with samples nor irradiated with UV spot. UV represents the UV group, that cells were treated with UV irradiation. Emu, L'Or, and Emu-G represent the emulsion, L'Oreal and emulsion gel groups, that cells were covered with the same amount of emulsion, L'Oreal sunscreen, and emulsion gel sample before UV irradiation, respectively.

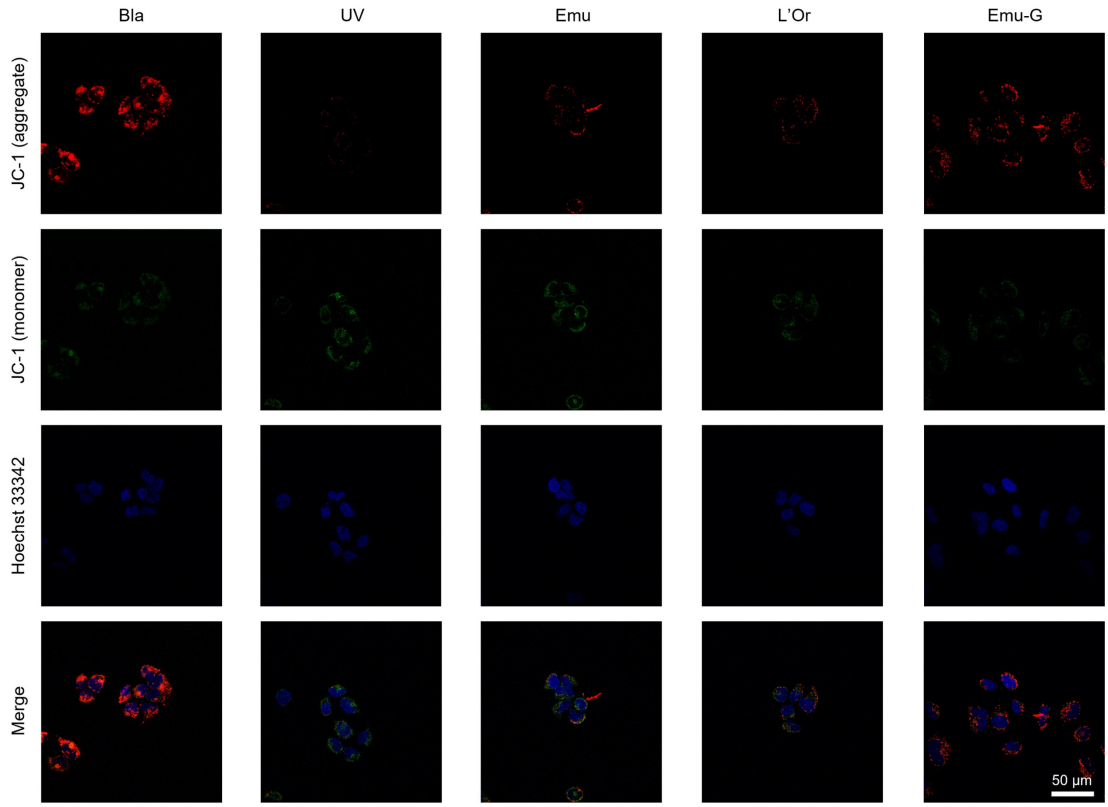

Supplementary Fig. 30. Effects of different samples protection on mitochondrial membrane depolarization induced by UV irradiation of HaCaT cells. Bla represents the blank group, that cells were neither covered with samples nor irradiated with UV spot. UV represents the UV group, that cells were treated with UV irradiation. Emu, L'Or, and Emu-G represent the emulsion, L'Oreal and emulsion gel groups, that cells were covered with the same amount of emulsion, L'Oreal sunscreen, and emulsion gel sample before UV irradiation, respectively. Red fluorescence indicates the mitochondrial aggregated form of JC-1 due to a high mitochondrial membrane potential ($\Delta\Psi m$), whereas green fluorescence represents the monomeric form of JC-1 due to low $\Delta\Psi m$, and blue fluorescence suggests the nuclei.

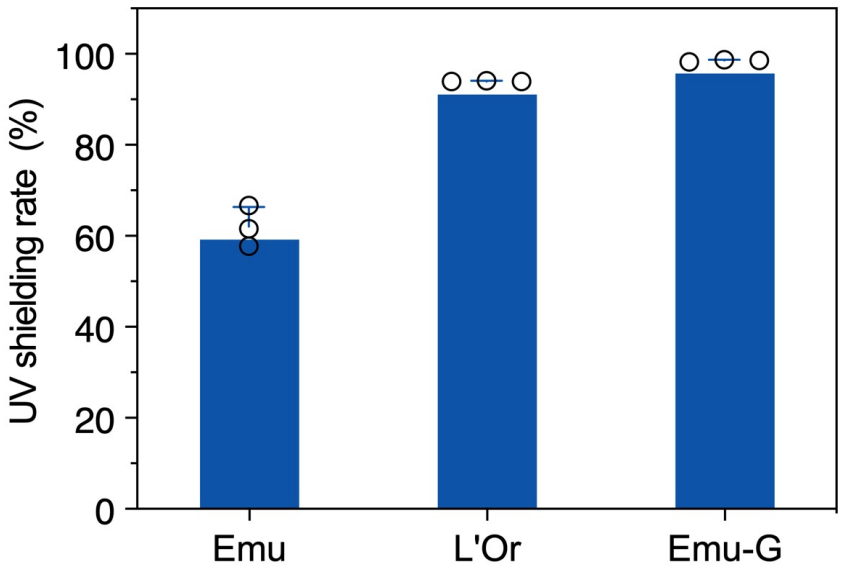

Supplementary Fig. 31. UV shielding rate of emulsion, L'Oreal sunscreen and emulsion gel samples. Data are presented as mean values ± SD (n = 3).

The results showed that the emulsion gels could effectively absorb/scatter > 98.5% UV light, while the UV-shielding rate of L'Oreal sunscreen and emulsion sample were 94.0% and 62.1%, respectively.

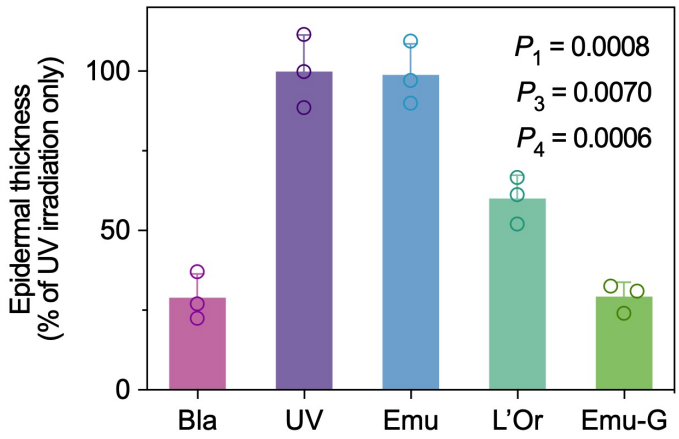

Supplementary Fig. 32. Relative epidermal thickness of mouse skin swabbed with different protective samples followed by UV irradiation. The epidermal thickness of the injured area was measured using ImageJ based on H&E staining images. Data were collected based on the normalization of the UV group (UV irradiation only sample) as 100% and presented as mean ± SD of n = 3 biologically independent mice.

The mouse skin of the UV group and the emulsion group exhibited a pronounced epidermal hypertrophy effect compared to the blank group (from 29% to 100% and 99%, respectively), which could be markedly diminished by L'Oreal sunscreen (epidermal thickness of 60%), whereas the thickness of emulsion gels-protected skins (29%) kept the original level with the blank.

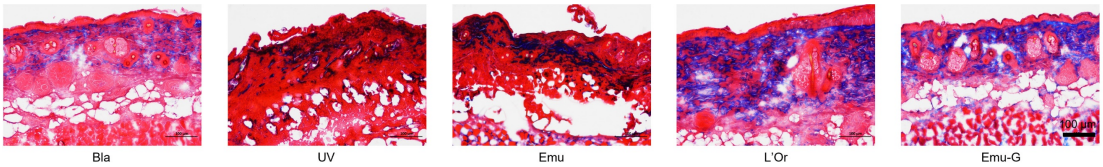

Supplementary Fig. 33. Trichrome staining of skin sections from the irradiated areas of five groups of mice collected on 3rd day.

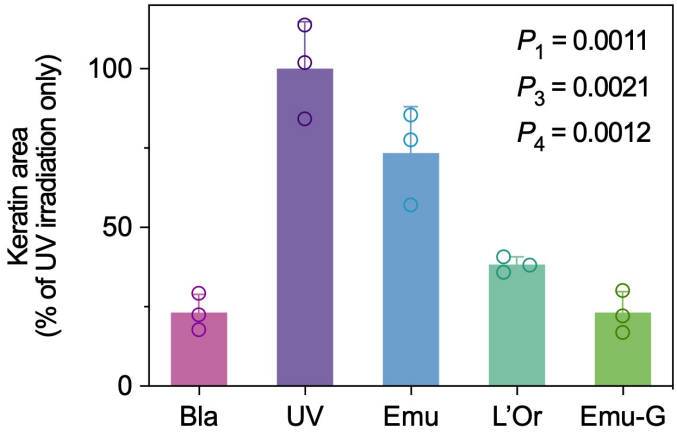

Supplementary Fig. 34. Relative keratin percentage of mouse skin swabbed with different protective samples followed by UV irradiation. The keratin percentage of the injured area was measured using ImageJ based on trichrome staining images. Data were collected based on the normalization of the UV group (UV irradiation only sample) as 100% and presented as mean ± SD of n = 3 biologically independent mice.

Compared with the blank group (23%), the skin tissues of mice demonstrated varied levels of keratin overproduction in the UV group, emulsion group, and L'Oreal group (100%, 73%, and 38%, respectively), while no discernible phenomena were observed in the skins coated with emulsion gels (23%).

Supplementary Table 1. The equivalent concentrations of samples that prepared with variations of volume mixing ratio between 4% *w*/*w* NP aqueous solution and toluene solution of 3% *w*/*w* PDMS-NH_2, if they are considered by mixing with 5:5.

Water/oil mixing ratio	Equivalent C_N	Equivalent C_P
8:2	6.4% *w*/*w* (= 4 × 8/5)	1.2% *w*/*w* (= 3 × 2/5)
7:3	5.6% *w*/*w* (= 4 × 7/5)	1.8% *w*/*w* (= 3 × 3/5)
6:4	4.8% *w*/*w* (= 4 × 6/5)	2.4% *w*/*w* (= 3 × 4/5)
5:5	4% *w*/*w* (= 4 × 5/5)	3% *w*/*w* (= 3 × 5/5)
4:6	3.2% *w*/*w* (= 4 × 4/5)	3.6% *w*/*w* (= 3 × 6/5)
3:7	2.4% *w*/*w* (= 4 × 3/5)	4.2% *w*/*w* (= 3 × 7/5)
2:8	1.6% *w*/*w* (= 4 × 2/5)	4.8% *w*/*w* (= 3 × 8/5)

Supplementary Table 2. The encapsulation rate and loading capacity of bridged emulsion gels as the carrier for β-carotene with different C_N. [C_P] = 3% *w*/*w*, water/oil ratio is 3:7 (*v*/*v*).

Different C_N	Encapsulation rate (%)	Loading capacity (μg/mg)
1 % *w*/*w*	97.03 ± 0.61	170.48 ± 1.07
2 % *w*/*w*	97.97 ± 0.47	86.07 ± 0.41
4 % *w*/*w*	98.69 ± 0.37	43.34 ± 0.16